Ray-optics model for optical force and torque on a spherical metal-coated Janus microparticle

Jing Liu,[1] Chao Zhang,[1] Yiwu Zong,[2] Honglian Guo,[1,3] and Zhi-Yuan Li[1,4]

[1]*Key Laboratory of Optical Physics, Institute of Physics, Chinese Academy of Sciences, Beijing 100190, China*
[2]*Key Laboratory of Soft Matter Physics, Institute of Physics, Chinese Academy of Sciences, Beijing 100190, China*
[3]*e-mail: hlguo@iphy.ac.cn*
[4]*e-mail: lizy@aphy.iphy.ac.cn*

In this paper, we develop a theoretical method based on ray optics to calculate the optical force and torque on a metallo-dielectric Janus particle in an optical trap made from a tightly focused Gaussian beam. The Janus particle is a 2.8 μm diameter polystyrene sphere half-coated with gold thin film several nanometers in thickness. The calculation result shows that the focused beam will push the Janus particle away from the center of the trap, and the equilibrium position of the Janus particle, where the optical force and torque are both zero, is located in a circular orbit surrounding the laser beam axis. The theoretical results are in good agreement qualitatively and quantitatively with our experimental observation. As the ray-optics model is simple in principle, user friendly in formalism, and cost effective in terms of computation resources and time compared with other usual rigorous electromagnetics approaches, the developed theoretical method can become an invaluable tool for understanding and designing ways to control the mechanical motion of complicated microscopic particles in various optical tweezers. © 2015 Chinese Laser Press

OCIS codes: (350.4855) Optical tweezers or optical manipulation; (170.4520) Optical confinement and manipulation.

http://dx.doi.org/10.1364/PRJ.3.000265

1. INTRODUCTION

Light carries momentum and energy. When a light beam illuminates an object, it produces radiation pressure on the object through the exchange of momentum with the object. In addition, when the light beam has some special spatial distribution of electromagnetic (EM) field intensity, a gradient force can be produced to pull the object toward the field gradient direction of the light beam. The coaction and balance of these two forces, the radiation force and gradient force, make it possible to form a three-dimensional (3D) optical potential well to trap the object in space. Optical tweezers [1], a technique pioneered by Ashkin [2], use a highly focused laser beam to implement 3D trapping of dielectric particles around the focus spot. This technique opens up a new regime to explore the undiscovered phenomena in biological [3–5], physical [6,7] and materials sciences and engineering areas [8]. In recent years, a variety of objects have been successfully trapped by optical tweezers, such as biconcave human red blood cells [9], gold nanoparticles [10–12], birefringent particles [13], and Janus particles [14–17].

It is well known that the optical forces strongly depend on the geometric and physical properties of the object under trapping. Theoretical and numerical analyses have become invaluable tools for better understanding the underlying physics and for deeper insight toward exploring novel ways to manipulate the mechanical motion of microscopic objects via optical forces. In this paper, we present a theoretical study of the optical forces on a polystyrene (PS) micrometer-sized spherical particle with a nanometer-thick gold thin film coating only half of its outer surface. This specific particle, in a broad aspect, belongs to an interesting family of so-called Janus particles. These particles, named after the double-faced Roman god, show two distinct physical, chemical, or other properties. They have found applications in Janus motors [18,19], switchable devices [20], and optical probes [21]. This class of asymmetric particles, when embedded within an optical trap, will exhibit interesting mechanical motion behaviors. For instance, Merkt *et al.* reported that a gold-coated Janus particle can move away from and rotate around the focus of the laser beam used to form an optical trap [17].

Recently, we also performed optical trapping of Janus particles by using a focused Gaussian beam and found a similar behavior of mechanical motion. The half Au-coated Janus particle under our theoretical and experimental study is a metallo-dielectric hybrid optical microstructure. The introduction of the Au-coating film would bring about unique mechanical properties under the optical trap that a usual single-composite spherical particle does not have. Quantitative knowledge of the optical force and torque on the Janus particle is helpful or even indispensable for deeply understanding the physical mechanism of its translation, rotation, and other mechanical motion behaviors. However, this requires extensive numerical computation because analytical solutions based on the well-known Mie's theory are not applicable to these asymmetric hybrid particles. Up to date, the quantitative theoretical analysis of mechanical motion of a Janus particle within optical tweezers is still blank; thus, it is the task of this work.

When the particle size is smaller than or close to the wavelength of light, some practical methods based on electromagnetism have been proposed to calculate the optical forces, including the finite element method [22], the finite-difference

time-domain (FDTD) method [23,24], the discrete dipole approximation [25,26], and the T-matrix method [27]. In the scenario of this paper, however, the particle diameter is so large (several micrometers) compared with the coated gold thin film (several nanometers). This drastic contrast in space scale for two distinctly different materials (metal versus dielectric) will cause a huge calculation burden. Taking the widely used method of FDTD as an example, the simulation area is needed to be 5 μm × 5 μm × 5 μm for a Janus particle 2.8 μm in diameter. Meanwhile, the mesh grid is required to be less than 1 nm in order to accurately reflect the interaction of the light beam and the metal film. Hence, the total cell number can be up to a huge number of 1.25×10^{11}, and the computation is far beyond the capacity of usual computers.

To lift this severe obstacle, other methods adopting a very different concept must be considered. In the early 1990s, Ashkin demonstrated that ray optics can give a reasonable and reliable theoretical value for the trapping force on the dielectric sphere with a diameter much larger than wavelength [28]. This simple ray-optics method, although an approximate model, works very well in comparison with experiments. Obviously, this method has a big advantage over rigorous electromagnetism simulation techniques in terms of computation resource and time. For this reason, we develop a theoretical method based on the ray optics to calculate the force and torque on a Janus particle in a trap, for which the usual electromagnetism methods are difficult to handle. To prove the feasibility of this method, we compare the theoretical and experimental results about the equilibrium position of the Janus particle in a trap. In addition, we give a reasonable explanation about the mechanical motion of the Janus particle in the trap.

The rest of this paper is organized as follows. In Section 2, we describe the computational procedures of the developed method. In Section 3, we make a comparison between theory and experiment and verify the feasibility of the proposed method. In Section 5, we conclude this paper.

2. THEORY AND FORMULATIONS FOR OPTICAL FORCES AND TORQUES

We consider calculation of the optical force and torque on the Janus particle in a trap from the perspective of momentum exchange, which should happen at each interaction point of the focused Gaussian beam with the surface of the particle. In the regime of ray optics, the focused Gaussian light beam is decomposed into a large amount of individual rays. At the interface of the particle and the surrounding medium, the rays are reflected and refracted, and sometimes they are absorbed by the particle. In this way, the momenta of light are transferred to the particle, creating optical force at each point. To quantitatively account for the momentum transfer, we employ the Fresnel formula to calculate the reflection, refraction, and absorption coefficients for each ray at each event of its intersection with the particle interface. Then, we calculate the momentum transfer and the corresponding interaction forces generated by the reflections, refractions, and absorptions of each ray at each interface. Finally, we sum up all these forces, which is the net force on the Janus particle in the trap. Following a similar procedure, we can calculate the net torque on this Janus particle by combining the force and position information at the entire surface of the particle.

As illustrated in Figs. 1(a) and 1(b), the Janus particle is the PS particle with radius r_s and half-coated with gold film of thickness h. In our practical experiments, the Janus particle is prepared by magnetron sputtering gold film normally onto PS microspheres. The thickness of gold film is then maximal at the top surface of the PS sphere and reduces gradually to zero at the position of equator, approximately following the relation of $h = h_0 \sin \psi$, where h_0 is the maximum thickness at the top of the PS particle, while ψ is the inclination angle of a particular point at the PS surface with respect to the y axis. The gold film configuration is rotationally symmetric with respect to the sputtering direction, which is designated as the y-axis direction in Figs. 1(a) and 1(b). The Janus particles are suspended in an aqueous solution in practical optical trapping experiments.

The single-beam optical trap is generated by a strongly focused Gaussian laser beam, which propagates along the z-axis direction. The Janus particle is initially oriented in such a way that the unit vector from the PS side to the metal side, namely, the normal vector of the metal-dielectric separation plane of the Janus particle, is parallel to the y axis. Due to the asymmetric feature, the Janus particle will experience the optical torque and rotate around the x axis. The orientation angle denoted by α is the rotational angle of the Janus particle around the x axis. The initial rotational angle is set to be zero.

A. General Concepts of the Ray-Optics Model
The coordinate system used for the calculation is shown in Fig. 1(c). The center of the Janus particle, point "O," is set as the coordinate origin. The collimated Gaussian beam at a wavelength of 1064 nm propagates along the z axis and is focused by a high NA microscope objective to a focal point located at $f = [f_x, f_y, f_z]$. The total light beam is decomposed within its cross section into a number of individual rays with appropriate intensity and propagation direction. The initial propagation directions of these rays are denoted by $\vec{k_1}, \vec{k_2}, \vec{k_3}, \ldots, \vec{k_n}, \ldots$ before they interact with the Janus particle. Here, the propagation direction $\vec{k_n}$ can be represented as $\vec{k_n} = [-r \sin \varphi, -r \cos \varphi, f_z]$. Note that all these directional vectors are normalized as a unit vector of norm 1.

In order to better describe the calculation of the total force, we first consider the force due to a single ray of a power P hitting the Janus particle at the propagation direction $\vec{k_1}$ with an incident momentum Pn_1/c per second, where n_1 is the refractive index of the aqueous solution, and c is the speed of light in vacuum. Note that the incident ray will be subject to multiple reflection and refraction events within the particle, and each time there will be momentum transfer and exchange between light and particle, generating optical force and torque. Then, the overall force $\vec{F} = [F_x, F_y, F_z]$ can be given by $\vec{F} = \vec{Q} \cdot Pn_1/c$, where $\vec{Q} = [Q_x, Q_y, Q_z]$ is a dimensionless factor that describes the momentum exchange coefficient of each ray interacting with the Janus particle and is associated with the overall reflection of the light beam. The factor $\vec{Q}$ is the sum of the reflected ray with directional strength $\vec{k_{1r}} R_1$, and the infinite number of emergent refracted rays of directional strength $\vec{k_{2t}} T_1 T_2, \vec{k_{3t}} T_1 R_2 T_3, \ldots, \vec{k_{nt}} T_1 T_n (R_2 \cdot R_3 \ldots R_{n-1}), \ldots$. The quantities T_n and R_n represent the Fresnel reflection and transmission coefficients at the nth intersection event of the transport ray with the particle surface. A diagram
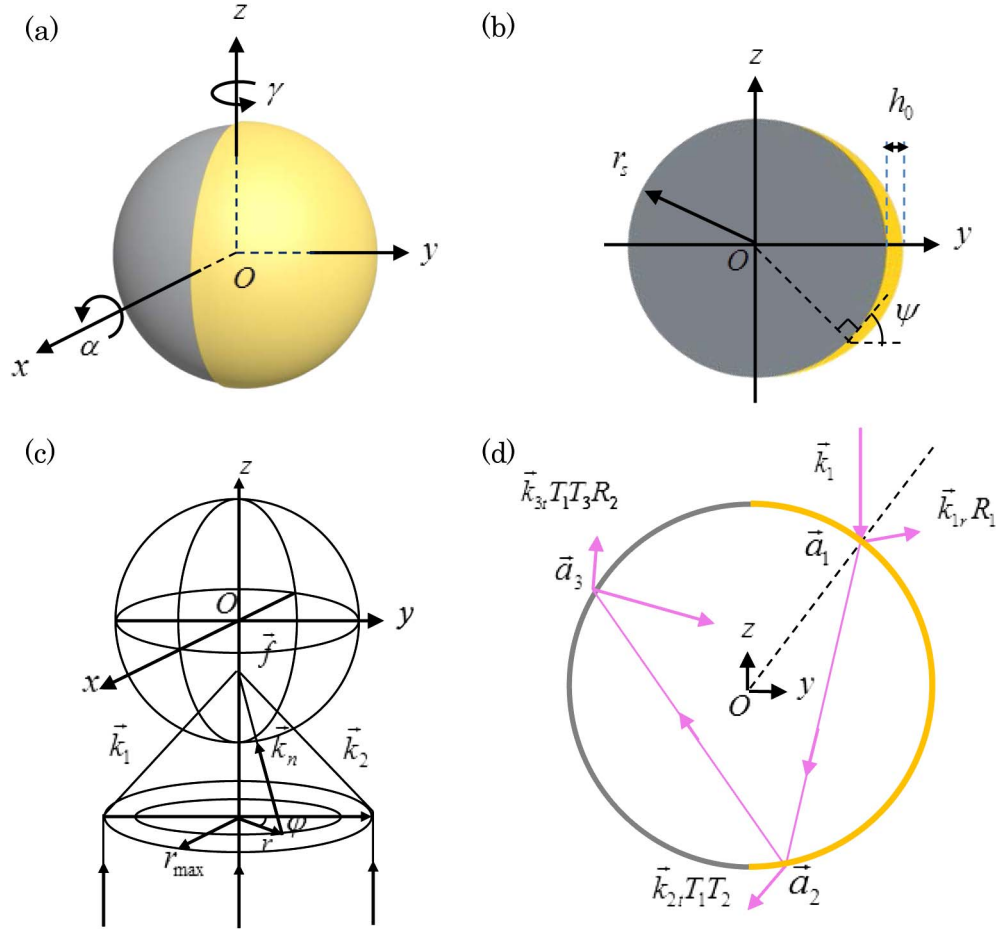
Fig. 1.   Diagram of ray-optics model used to handle trapping and motion of Janus particles in a tightly focused Gaussian laser beam. (a) 3D stereogram of the Janus particle made from a PS bead half-coated with thin gold film. The Au–PS separation plane of the particle can rotate around the axis of laser beam (z axis, denoted by the angle γ), and the orientation of its surface normal vector with respect to the laser beam axis can change (denoted as by the angle α). (b) Schematic diagram of the cross-sectional geometry of the Janus particle in the plane of $x = 0$. The gold thin film thickness reduces gradually from the top of the PS bead (the y-axis direction) to the separation plane (the x–z plane). (c) Diagram of a Gaussian laser beam tightly focused by a high-NA microscope objective lens with pupil radius r_{max} and illuminating the Janus particle for optical trapping and manipulation. In the ray-optics model, the laser beam is decomposed into a large amount of rays of light denoted by their directional unit vectors $\vec{k}_1, \vec{k}_2, \vec{k}_3, \ldots, \vec{k}_n, \ldots$. The k_i ray intersects with the objective pupil at the position with polar coordinate $\vec{r}_i = (r, \varphi)$. (d) Diagram of the ray tracking for a specific ray $\vec{k}_1$ within the Janus particle, where multiple events of ray reflection and refraction will take place at the positions $\vec{a}_1, \vec{a}_2, \vec{a}_3$, etc. Momentum exchange and transfer at each event can be calculated to yield the optical force and torque, all of which will sum up to yield the net total force and torque by the laser beam upon the Janus particle.

of the above mechanical analysis in the regime of ray optics is illustrated in Fig. 1(d) in detail for clarity. The general framework of the above ray-optics theoretical model and calculation formalism is composed of the following important elements.

B. Computational Procedures
The proposed ray-optics method consists of the following six steps:

1. Check whether the intersection and interaction point exists for a particular ray of light. If the ray and the Janus particle do not intersect, then no interaction occurs and $\vec{Q} = [0, 0, 0]$. If the intersection and interaction occur, go to step 2. Otherwise, go to step 5.

2. Calculate the coordinate value (x_1, y_1, z_1) of the interaction point $\vec{a}_1$ and determine which side (the Au surface or the PS surface) the incident ray reaches.

3. Calculate the Fresnel reflection and transmission coefficients at the interaction position, assuming a locally flat

surface for the incident ray. The transmission coefficient is denoted by T, and the reflection coefficient is denoted by R. These two quantities are normalized to the incident ray strength. If $R < 10^{-15}$, which means that the ray strength at this specific interaction has been extremely weak and can be negligible, go to step 5.

4. Track the ray. When an interaction occurs, go to step 2; otherwise, go to step 5.

5. End the iteration. Calculate and output the net optical force and torque from all the above R and T for the particular ray of light, which is the vector sum of all the forces and torques.

6. Repeat the above five procedures for all rays of light. Calculate the total net optical force and torque for the whole incident Gaussian beam upon the Janus particle.

C. Calculation of Reflection and Transmission Coefficients
We proceed to discuss the details of the above procedure, where R and T are the key values for characterizing the

precise quantity of momentum exchange and transfer. Due to the special metal film coating on the Janus particle, the reflection of light on the Au surface (namely, the water–Au interface) is much stronger than that on the PS surface (namely, the water–PS interface). This kind of difference will result in the different behavior between the PS particle and Janus particle. In this paper, we use the well-known Fresnel formulae [29] to calculate R and T.

1. Polystyrene Surface

If the ray hits the PS surface, we only need to consider the single interface of water and PS. The schematic configuration of light transport with the incident angle θ_1 and the refraction angle θ_3 is shown in Fig. 2(a). The refractive indices of water and PS are represented by n_1 and n_3, respectively. The method of calculating R and T varies with the polarization state of the incident ray. Hence, the electric field vector of the incident ray is separated into the vertical vector and parallel vector with respect to the incident plane.

If the electric field vector is perpendicular to the plane of incidence (*s*-polarized light), the reflection and transmission intensity coefficients are given by

$$R_E = \left[\frac{n_1 \sin\theta_1 - n_3 \cos\theta_3}{n_1 \sin\theta_1 + n_3 \cos\theta_3} \right]^2,$$

$$T_E = \frac{n_3 \cos\theta_3}{n_1 \cos\theta_1} \left[\frac{2n_1 \sin\theta_1}{n_1 \sin\theta_1 + n_3 \cos\theta_3} \right]^2. \tag{1}$$

On the contrary, if the electric field vector is parallel to the plane of incidence (*p*-polarized light), the reflection and transmission intensity coefficients are given by

$$R_M = \left[\frac{n_3 \cos\theta_1 - n_1 \cos\theta_3}{n_3 \cos\theta_1 + n_1 \cos\theta_3} \right]^2,$$

$$T_M = \frac{n_1 \cos\theta_3}{n_3 \cos\theta_1} \left[\frac{2n_3 \cos\theta_1}{n_3 \cos\theta_1 + n_1 \cos\theta_3} \right]^2. \tag{2}$$

2. Au Surface

When the ray hits the Au surface, we need to consider the two-interface problem consisting of water, gold film, and PS, as illustrated in Fig. 2(b). Let $\hat{n}_2 = n_2 + ik_2$ be the complex refractive index of gold and define $\hat{n}_2 \cos\theta_2 = u_2 + iv_2$, where u_2 and v_2 are real numbers, for the sake of calculation convenience. The value of θ_2, u_2, and v_2 can be easily calculated from Snell's law under an incident angle θ_1.

For the *s*-polarized light, we obtain

$$R_E = |r|^2 = \frac{\rho_{12}^2 e^{2v_2\eta} + \rho_{23}^2 e^{-2v_2\eta} + 2\rho_{12}\rho_{23}\cos(\phi_{23} - \phi_{12} + 2u_2\eta)}{e^{2v_2\eta} + \rho_{12}^2\rho_{23}^2 e^{-2v_2\eta} + 2\rho_{12}\rho_{23}\cos(\phi_{23} + \phi_{12} + 2u_2\eta)}, \tag{3}$$

$$T_E = \frac{n_3 \cos\theta_3}{n_1 \cos\theta_1}|t|^2 = \frac{n_3 \cos\theta_3}{n_1 \cos\theta_1}$$
$$\times \frac{\tau_{12}^2\tau_{23}^2 e^{-2v_2\eta}}{1 + \rho_{12}^2\rho_{23}^2 e^{-4v_2\eta} + 2\rho_{12}\rho_{23}e^{-2v_2\eta}\cos(\phi_{23} + \phi_{12} + 2u_2\eta)}. \tag{4}$$

In the above equations, the unknown parameters are given as follows:

$$\rho_{12}^2 = \frac{(n_1 \cos\theta_1 - u_2)^2 + v_2^2}{(n_1 \cos\theta_1 + u_2)^2 + v_2^2}, \quad \tan\phi_{12} = \frac{2v_2 n_1 \cos\theta_1}{u_2^2 + v_2^2 - n_1^2\cos^2\theta_1},$$

$$\rho_{23}^2 = \frac{(n_3 \cos\theta_3 - u_2)^2 + v_2^2}{(n_3 \cos\theta_3 + u_2)^2 + v_2^2}, \quad \tan\phi_{23} = \frac{2v_2 n_3 \cos\theta_3}{u_2^2 + v_2^2 - n_3^2\cos^2\theta_3}.$$

In Eqs. (3) and (4), $\eta = 2\pi h/\lambda_0$, where h is the thickness of the coated metal film, and λ_0 is the wavelength of the incident beam, which is 1064 nm here.

For the *p*-polarized light, we can derive the reflection and transmission intensity coefficients with similar mathematical manipulations. The results are

$$R_M = |r|^2 = \frac{\rho_{12}^2 e^{2v_2\eta} + \rho_{23}^2 e^{-2v_2\eta} + 2\rho_{12}\rho_{23}\cos(\phi_{23} - \phi_{12} + 2u_2\eta)}{e^{2v_2\eta} + \rho_{12}^2\rho_{23}^2 e^{-2v_2\eta} + 2\rho_{12}\rho_{23}\cos(\phi_{23} + \phi_{12} + 2u_2\eta)}, \tag{5}$$

$$T_M = \frac{n_1 \cos\theta_3}{n_3 \cos\theta_1}|t|^2 = \frac{n_1 \cos\theta_3}{n_3 \cos\theta_1}$$
$$\times \frac{\tau_{12}^2\tau_{23}^2 e^{-2v_2\eta}}{1 + \rho_{12}^2\rho_{23}^2 e^{-4v_2\eta} + 2\rho_{12}\rho_{23}e^{-2v_2\eta}\cos(\phi_{23} + \phi_{12} + 2u_2\eta)}. \tag{6}$$

The other unknown parameters are given as follows:

$$\rho_{12}^2 = \frac{[n_2^2(1 - \kappa_2^2)\cos\theta_1 - n_1 u_2]^2 + [2n_2^2\kappa_2 \cos\theta_1 - n_1 v_2]^2}{[n_2^2(1 - \kappa_2^2)\cos\theta_1 + n_1 u_2]^2 + [2n_2^2\kappa_2 \cos\theta_1 + n_1 v_2]^2},$$

$$\tan\phi_{12} = 2n_1 n_2^2 \cos\theta_1 \frac{2\kappa_2 u_2 - (1 - \kappa_2^2)v_2}{n_2^4(1 + \kappa_2^2)^2\cos^2\theta_1 - n_1^2(u_2^2 + v_2^2)},$$

$$\tau_{12}^2 = \frac{4n_2^4(1 + \kappa_2^2)^2\cos^2\theta_1}{[n_2^2(1 - \kappa_2^2)\cos\theta_1 + n_1 u_2]^2 + [2n_2^2\kappa_2 \cos\theta_1 + n_1 v_2]^2},$$

$$\rho_{23}^2 = \frac{[n_2^2(1 - \kappa_2^2)\cos\theta_3 - n_3 u_2]^2 + [2n_2^2\kappa_2 \cos\theta_3 - n_3 v_2]^2}{[n_2^2(1 - \kappa_2^2)\cos\theta_3 + n_3 u_2]^2 + [2n_2^2\kappa_2 \cos\theta_3 + n_3 v_2]^2},$$

$$\tan\phi_{23} = 2n_3 n_2^2 \cos\theta_3 \frac{2\kappa_2 u_2 - (1 - \kappa_2^2)v_2}{n_2^4(1 + \kappa_2^2)^2\cos^2\theta_3 - n_3^2(u_2^2 + v_2^2)},$$

$$\tau_{23}^2 = \frac{4n_3^2(v_2^2 + u_2^2)}{[n_3 u_2 + n_2^2(1 - \kappa_2^2)\cos\theta_3]^2 + (n_3 v_2 + 2n_2^2\kappa_2 \cos\theta_3)^2}.$$

In the end, the overall transmission coefficient T and reflection coefficient R are given by $T = (T_E + T_M)/2$ and
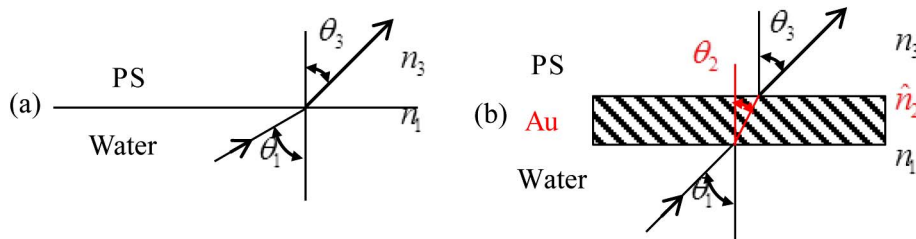

Fig. 2.   Sketch of the propagation of a ray on (a) the PS surface and (b) the Au surface. Reflection and refraction of the ray happen, and the corresponding intensity reflection and transmission coefficients can be calculated based on Fresnel's formulae.

$R = (R_E + R_M)/2$, when considering the rotational symmetry of the current optical problem involving spherical PS particles.

D. Calculation of Optical Forces and Torques

Tracking the ray transport is another important step in the calculation procedure. The incident light direction vector $\vec{k}_1 = (k_x, k_y, k_z)$ is already known, the direction vector of the first reflection ray of light is denoted as $\vec{k}_{1r}$, and the direction vector of the nth transmission ray of light is denoted as $\vec{k}_{nt}$. All the above reflection and transmission direction vectors can be straightforwardly derived from the law of reflection and Snell's law. Again, all these directional vectors are normalized as unit vectors. The overall force contributed by this ray can be calculated via the principle of the exchange of momentum as

$$\vec{F}_{k_1} = \frac{Pn_1}{c}\left(\vec{k}_1 - \vec{k}_{1r}R_1 - \vec{k}_{2t}T_1T_2 - \sum_{n=3}^{\infty}\vec{k}_{nt}T_1T_n(R_2 \cdot R_3 \dots R_{n-1})\right)$$
$$= \frac{Pn_1}{c}\vec{Q}_{k_1}. \tag{7}$$

The total force imposed upon the Janus particle by the focused Gaussian beam is simply the vector sum over the force of all rays of light:

$$\vec{F}_{\text{total}} = \sum_{i=1}^{N}W_{k_i}\vec{F}_{k_i} = \frac{Pn_1}{c}\sum_{i=1}^{N}W_{k_i}\vec{Q}_{k_i}. \tag{8}$$

Here, W_{k_i} is the weight of contribution parameter of the k_i ray of light, which is proportional to the intensity profile of the incident Gaussian beam in the entrance pupil of the high-NA lens, and N is the total number of rays considered in the calculation. This means that the central rays have the largest weight of contribution, while the rays at the edge of the pupil have the smallest weight of contribution. The variation of weight from the center to the edge follows a simple Gaussian distribution function.

In a similar way, the torque of a ray and the total torque of the Gaussian beam on the Janus particle can be calculated as follows:

$$\vec{\tau}_{k_1} = \frac{Pn_1}{c}[(\vec{a}_1 - \vec{S}) \times \vec{k}_1 - (\vec{a}_2 - \vec{S}) \times \vec{k}_{1r}R_1 - (\vec{a}_3 - \vec{S}) \times \vec{k}_{1r}\vec{k}_{2t}T_1T_2$$
$$- \sum_{n=3}^{\infty}(\vec{a}_n - \vec{S}) \times \vec{k}_{nt}T_1T_n(R_2 \cdot R_3 \dots R_{n-1})] = \frac{Pn_1}{c}\vec{M}_{k_1}, \tag{9}$$

$$\vec{\tau}_{\text{total}} = \sum_{i=1}^{N}W_{k_i}\vec{\tau}_{k_i} = \frac{Pn_1}{c}\sum_{i=1}^{N}W_{k_i}\vec{M}_{k_i}. \tag{10}$$

Here, the vector $\vec{S}$ denotes the position vector of the focus spot center of the Gaussian beam, and, as such, the torque of the Janus particle is measured with respect to the focus spot.

In the above equations, the force and torque are related to the power P of each ray of light comprising the incident laser beam. In experiments, this parameter can be connected with the total power P_{total} of the laser beam entering the pupil of objective lens by

$$P = P_{\text{total}}\frac{r\Delta\varphi \cdot \Delta r}{\pi r_{\max}^2} \tag{11}$$

for the ray of light (with directional vector $\vec{k}_i$) hitting the objective lens at the position with polar coordinate $\vec{r}_i = (r, \varphi)$. Here, the power density of the incident laser beam within the objective lens is estimated as $P = P_{\text{total}}/(\pi r_{\max}^2)$, where $r_{\max}$ is the maximum radius of the objective pupil. The total force and torque of the laser beam on the Janus particle are then correlated with the total power of the beam by rewriting Eqs. (8) and (10) into

$$\vec{F}_{\text{total}} = \frac{P_{\text{total}}n_1}{c}\sum_{i=1}^{N}W_{k_i}\vec{Q}_{k_i}\frac{r_{k_i}\Delta\varphi \cdot \Delta r}{\pi r_{\max}^2}, \tag{12}$$

$$\vec{\tau}_{\text{total}} = \frac{P_{\text{total}}n_1}{c}\sum_{i=1}^{N}W_{k_i}\vec{M}_{k_i}\frac{r_{k_i}\Delta\varphi \cdot \Delta r}{\pi r_{\max}^2}. \tag{13}$$

It can be seen that the total force and torque are proportional to the total power (or, equivalently, the average power density) of the laser beam. Other factors contributing to the force and torque include the size and geometry of the Janus particle, the NA of objective lens, and the refractive index of the PS bead. These physical and geometric parameters determine the mechanical motion behaviors of the Janus particle in the optical trap. The total torque $\vec{\tau}_{\text{total}} = [\tau_x, \tau_y, \tau_z]$ can be written alternatively as $\vec{\tau}_{\text{trap}} = \vec{M} \cdot P_{\text{total}}n_1/c$, where $\vec{M} = [M_x, M_y, M_z]$. Based on the above analysis, we can obtain the force and torque of a Janus particle in an arbitrary position.

3. CALCULATION RESULTS AND DISCUSSIONS

For a dielectric sphere, the stable equilibrium point $\vec{S} = [S_{x0}, S_{y0}, S_{z0}]$ can be calculated under the condition of $\vec{F}_{\text{total}} = [0, 0, 0]$. This equilibrium position is related to the translational motion of the particle. However, the situation is different for a Janus particle due to its asymmetric structure. The torque is connected with the orientation angle. A half-Au-coated Janus particle does not necessarily reach equilibrium if only the condition of $\vec{F}_{\text{total}} = [0, 0, 0]$ is matched. Because nonzero torque ($\vec{\tau}_{\text{total}} \neq [0, 0, 0]$) will lead to the rotation of the Janus particle in the trap, it will eventually modify the translational-motion equilibrium position of the particle. Hence, the stable equilibrium point $\vec{S} = [S_{x0}, S_{y0}, S_{z0}]$ should be obtained under the condition of $\vec{F}_{\text{total}} = [0, 0, 0]$ and $\vec{\tau}_{\text{total}} = [0, 0, 0]$ for the translational and rotational motions of the particle.

The parameters we used in the calculation are as follows. The PS bead has a diameter of 2.8 μm and is half-coated with gold film 3.5 nm in maximum thickness, i.e., $h_0 = 3.5$ nm. The numerical aperture of objective is NA = 1.4, $n_1 = 1.33$, $n_3 = 1.6$, and $\hat{n}_2 = 0.0963 + 6.3317i$ for gold at the wavelength of 1064 nm. The incident Gaussian beam propagates along the z direction. Figure 3(a) shows the calculated dependence of R and T on the incident angle θ_1, where θ_1 varies from 0° to 90° for a simplified model system where the gold thin film has a fixed thickness of 0, 2, or 4 nm everywhere in the half sphere. The result shows that the reflection of the gold film layer is much higher than that of the PS layer when the angle is small, which means the momentum exchange from the light beam to the gold film layer is higher than that of the PS layer. This strongly asymmetric reflection property at the PS half sphere and the gold half sphere could lead to an unbalanced scattering force, and the net force would
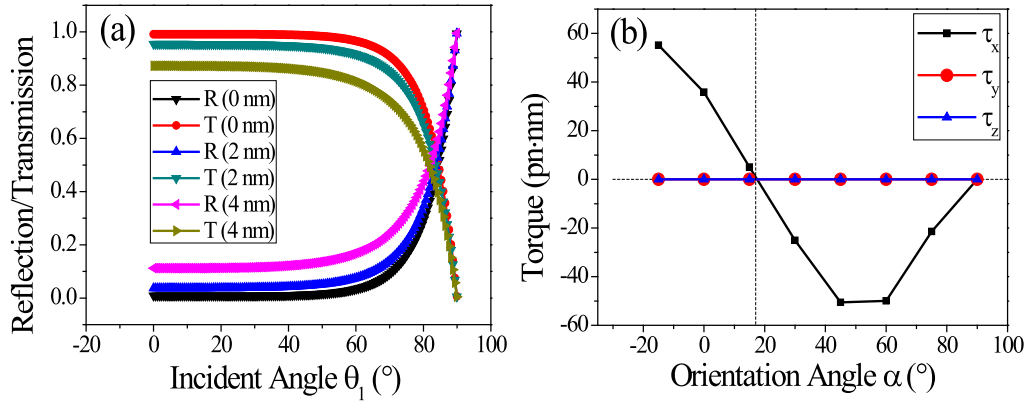
Fig. 3.   (a) Calculated intensity reflection and transmission coefficients as a function of the incident angle θ_1 on the gold thin film layer with the thickness of 0, 2, and 4 nm, respectively. (b) Calculated optical torques of laser beam upon the Janus particle as a function of the orientation angle α of the Au–PS separation plane.

point from the gold side to the PS side if the Janus particle is fixed exactly at the focus spot center. Of course, because the Janus particle is free, it will be pushed by this net force and move along this direction until reaching an equilibrium position somewhere away from the focus spot center of the Gaussian beam.
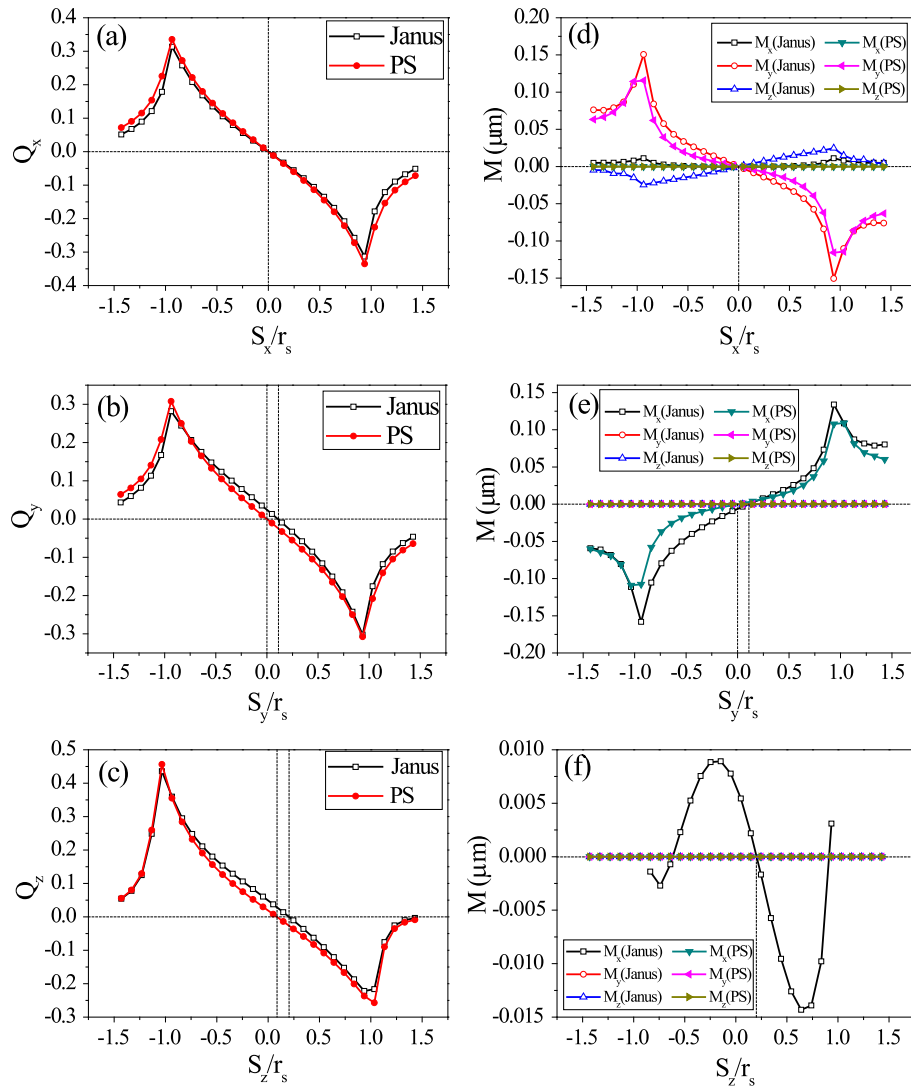

Fig. 4.   Comparison of the optical force and torque on a Janus particle with those on a PS particle imposed by the focused laser beam. (a) Sketch of $Q_x \sim (S_x/r_s)$. (b) Sketch of $Q_y \sim (S_y/r_s)$. (c) Sketch of $Q_z \sim (S_z/r_s)$. (d) Sketch of $M \sim (S_x/r_s)$. (e) Sketch of $M \sim (S_y/r_s)$. (f) Sketch of $M \sim (S_z/r_s)$.

In order to get the point where $\vec{\tau}_{\text{total}} = [0, 0, 0]$, we vary the orientation angle α in the range from $-15°$ to $90°$ and calculate $\vec{\tau}_{\text{total}}$ at each value of α. As has been illustrated in Fig. 1(a), the orientation angle α describes the relative posture of the asymmetric Janus particle, in particular, its separation plane orientation with respect to the axis of the Gaussian beam. $\alpha = 0°$ means that the separation plane is parallel to the beam axis, while $\alpha = 90°$ means that the separation plane is perpendicular to the beam axis. As shown in Fig. 3(b), the total torque against the Janus particle reaches zero at the orientation angle of $\alpha = 17°$. This orientation angle is stable because any angular deviations from this orientation angle will be countered by restoring torque. When the orientation angle of the Janus particle is confirmed, we can go further to find out the equilibrium position under the condition that the total force $\vec{F}_{\text{total}} = [0, 0, 0]$.

To clearly show this point, we display the calculated force and torque as a function of the position and orientation of the Janus particle around the identified equilibrium position in Fig. 4. For the sake of comparison, we also plot in Fig. 4 the force and torque of the PS spherical bead. Comparison between them illustrates the clearly distinct mechanical properties of these two particles in the optical trap. It can be seen in Figs. 4(a)–4(c) that the equilibrium position of the PS bead is $[0, 0, 0.08r_s]$ when interacting with the optical trap. This means that the PS bead is trapped at the laser beam axis with zero lateral offset and has a small longitudinal offset along the laser beam propagation direction due to the scattering force.

The equilibrium position of the Janus particle is $[0, 0.107r_s, 0.2r_s]$, with the value of S_{y0} equal to $0.107r_s$. This means that the optical force tends to push the Janus particle outward with a distance from the laser beam axis of $0.107r_s$, which is about 150 nm. This lateral offset from the focus spot center is attributed to the asymmetric scattering force by the laser beam hitting on the gold side and the PS side, with the former much larger than the latter. Meanwhile, in Fig. 4(c), the longitudinal offset of the Janus particle along the laser beam propagation direction ($+z$ axis) is much higher than that of the PS bead. This is again attributed to the much larger overall scattering force of the laser beam induced by the much stronger reflection of light by the gold film and larger momentum transfer. This large longitudinal offset also indicates that the Janus particle is less stable than the PS sphere because it is far away from the focus spot center. With increasing thickness of the gold film layer, the offset becomes larger and larger. If the force in the z direction keeps being greater than zero, then the S_{z0} does not exist. In this case, the optical trap cannot trap the Janus particle three dimensionally.

In addition, we compare the torque of the Janus particle with that of the PS spherical bead in Figs. 4(d)–4(f). Whether for the Janus particle or the PS spherical bead, the equilibrium positions when the torque $\vec{\tau}_{\text{total}} = [0, 0, 0]$ and the force $\vec{F}_{\text{total}} = [0, 0, 0]$ are the same—and they are stable at each equilibrium position. Furthermore, through scanning the light beam focus along the x, y, and z axes, the torque of the PS spherical bead in the z axis is invariably equal to zero, which means that it is impossible to observe the rotation of the PS spherical bead in a single laser beam. However, when the Janus particle enters into the laser beam from outside, the Janus particle can obtain the torque in the z direction, as shown in Fig. 4(d), which can support its rotation.
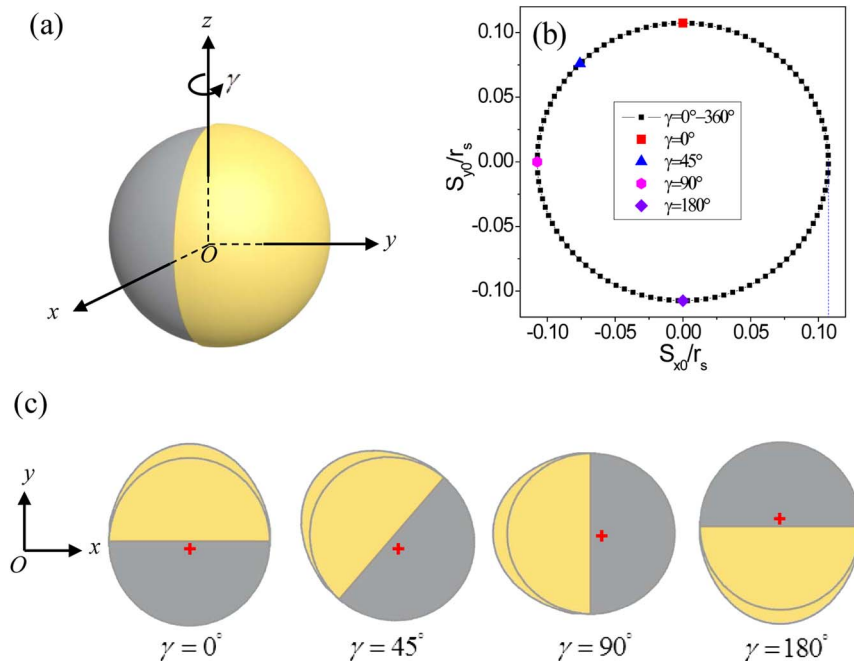

Fig. 5. (a) 3D stereogram of the asymmetric Janus particle with its separation plane rotating around the axis of a laser beam denoted by the angle γ. (b) Calculated equilibrium positions of the Janus particle in the x–y plane as γ varies, which are located at a circle $0.107\ r_s$ in distance from the axis of the laser beam. (c) Plane graph of the Janus particle posture with respect to the laser beam axis when $\gamma = 0°, 45°, 90°, 180°$. The corresponding equilibrium positions of the particle are explicitly marked in panel (b) by colored dot signals. In each case, the equilibrium position, which is also the center of the Janus particle, when measured with respect to the laser beam axis (denoted by the red-cross signal), remains fixed with the same later offset distance. This further confirms the result of panel (b) that the center of the Janus particle will rotate around the laser beam axis in a fixed distance.
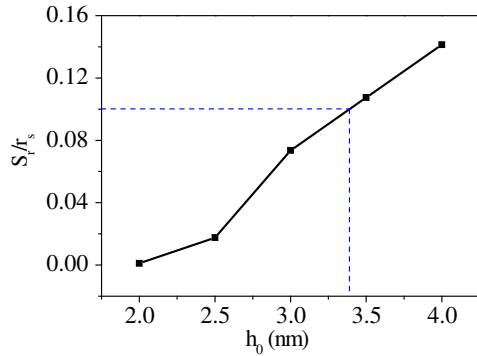
Fig. 6.   Calculated distance of the equilibrium positions of the Janus particle away from the laser beam axis with variation of the thickness of gold film.

4. COMPARISON WITH EXPERIMENTS

Another issue concerning the mechanical motion of the Janus particle is its rotation around the laser beam axis, as was experimentally reported in [17]. To see whether this is reasonable in physics, we have made many more calculations by changing the rotation angle γ of the Janus particle, following the geometric configuration, as shown in Fig. 5(a). The situation of $\gamma = 0°$ has been considered in the above numerical calculations, as illustrated in Fig. 4, where the Janus particle center has an offset away from the laser beam axis along the y-axis direction, namely, with $[S_{x0}, S_{y0}] = [0, S_r]$. These calculations show that, at each value of γ, there is always a lateral offset of the particle center with respect to the laser beam axis, which is measured by $[S_{x0}, S_{y0}]$. Moreover, the absolute value of all the offset is the same, namely, $S_{x0}^2 + S_{y0}^2 = S_r^2$, so that the Janus particle center is located at a circle (with radius of S_r) surrounding the laser beam axis, as shown in Fig. 5(b). In addition, there always exists a longitudinal offset along the laser beam propagation direction in all rotational angles, and the value is the same. The position of Janus particle's center, which is also the equilibrium position of the particle in terms of force and torque, keeps fixed relatively when measured with respect to the Au–PS separation plane. The situation can be clearly seen in Fig. 5(c).

Further calculations are made by changing the gold film thickness. The results are plotted in Fig. 6 for the dependence of the lateral offset distance S_r on the maximum gold film thickness h_0. It is clear that the offset distance increases when the gold film becomes thicker. This is a natural result because the reflection in the gold side becomes larger; thus, the momentum exchange in the gold side and PS side differs more. As a result, the scattering force asymmetry gets more pronounced at thicker gold film, leading to a larger lateral offset distance of the particle center from the laser beam axis.

We also have performed similar experiments with Janus particles and found phenomena similar to [17] and consistent to our above theoretical calculations. The geometrical and physical parameters of Janus particles used in our experiment are consistent with (but surely not identical to) those used in the above calculations. They are loaded between two cover glasses and sealed using optical glue (Norland 65). An optical trap is generated by focusing an infrared Gaussian beam laser (Nd:YVO$_4$, Coherent Compass 1064 nm) with an oil-immersion objective (Leica, HCX PL APO, ×100, NA = 0.7–1.4). The laser power entering the objective was measured to be 57 mW.

A typical optical microscopy image of a Janus particle trapped by the optical tweezers in the experiment as recorded by a CCD is shown in Fig. 7(a). A black-white separation line existing within the Janus particle in this picture is clearly seen. This line simply corresponds to the Au–PS separation plane, which is dominantly but not exactly parallel to the axis of the focused laser beam. Furthermore, when a Janus particle was captured by the optical trap, it started to rotate clockwise or counterclockwise stably around the optical axis of the focused laser. The evidence is that, in optical microscopy, the black-white separation line rotated around the laser beam axis. We have recorded many events of the Janus particle position. The recorded data for the Janus particle center are displayed in Fig. 7(b). To facilitate convenience of eye view, we fit the data and find that the Janus particle center, on average, resides in a circle surrounding the laser beam axis. The radius of this circle simply corresponds to the averaged lateral offset of the Janus particle center due to the optical trap, as defined by $S_r = [S_{x0}^2 + S_{y0}^2]^{1/2}$. According to Fig. 5(b), this radius is about $0.102r_s$, which is close to the theoretical calculation
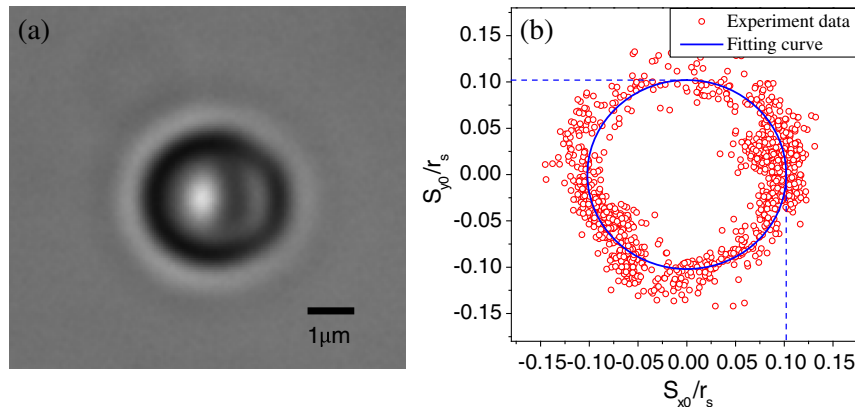

Fig. 7.   Experimental results of Janus particle trapping and motion within an optical tweezers produced from a Gaussian laser beam focused by a NA = 1.4 microscope objective lens. (a) Typical optical microscopy image of a Janus particle observed in experiments. The separation plane of the PS side (bright part) and gold side (dark part) particle can be clearly recognized, indicating that the Au–PS separation plane is dominantly parallel to the laser beam axis, which is normal to the paper sheet. (b) Recorded positions of the Janus particle center relative to the laser beam axis (where the optical trap center resides), which is set to locate at the origin of coordinates. The blue curve is the fitting averaged circular orbit where the center of the Janus particle resides when it rotates around the laser beam axis.

value of $0.107r_s$, as discussed in Figs. 4 and 5 for $h_0 = 3.5$ nm. More accurately, the offset distance $0.102r_s$ should correspond with the Janus particle with a gold film thickness of $h_0 = 3.4$ nm. In Fig. 7(b), one also can see quite a large fluctuation of the particle center around the averaged circular orbit. This can be attributed to the Brownian motion of the Janus particle as well as the instability of the optical tweezers system. However, overall good agreement between calculation and experiment results has been observed—not only qualitatively but also quantitatively. This agreement strongly supports the effectiveness and efficiency of the proposed ray-optics method in application to the new class of metallo-dielectric Janus particles.

5. CONCLUSION

In summary, we have developed a theoretical method based on a ray-optics model to calculate the optical force and torque on a half-Au-coated PS micrometer-sized spherical Janus particle trapped in optical tweezers. The calculations show that the coated gold thin film greatly increases the reflection upon light, so that the Janus particle obtains more momentum exchange and transfer from the laser beam on the gold side than on the PS side. As a consequence, the scattering force on the gold side is much larger than on the PS side. This asymmetric optical force will push the Janus particle away from the laser beam axis laterally to a new equilibrium position in terms of optical force and torque. In addition, the Janus particle will rotate around the laser beam axis along a circular orbit whose radius increases when the thickness of gold film increases. The calculation results are in good agreement with experimental observation made by our group and other researchers. This qualitative and quantitative agreement indicates that the simple ray-optics model is effective and efficient when it is applied to solve the mechanical motion of a complicated metallo-dielectric Janus particle ignited by optical forces and torques.

Because the ray-optics approach is much more user friendly than other rigorous EM simulation methods in regard to computational resources, time, and costs, it is expected that this simple while powerful approach can open up a new avenue in order to understand the mechanical motions within optical tweezers on the basis of quantitative calculation of the optical forces and torques. These particles can have complicated geometric and physical configurations, with the Janus particle being a prominent example. Besides, the optical tweezers can be made from either focused Gaussian beams or other beams such as focused line beams, Bessel beams, cylindrical vector beams, and so on. The ideas and insights accumulated via these theoretical studies can stimulate novel ways of optical tweezers engineering to manipulate the mechanical motion, including translational, rotational, and spinning motions of microscopic particles in a designated way that can be fascinating for applications in the areas of biology, physiology, physics, chemistry, nano-sciences, and nanotechnologies.

ACKNOWLEDGMENT

REFERENCES

1. H. L. Guo and Z. Y. Li, "Optical tweezers technique and its applications," Sci. China Phys. Astro. & Mech. **56**, 2351–2360 (2013).
2. A. Ashkin, J. M. Dziedzic, J. E. Bjorkholm, and S. Chu, "Observation of a single-beam gradient force optical trap for dielectric particles," Opt. Lett. **11**, 288–290 (1986).
3. M. D. Wang, H. Yin, R. Landick, J. Gelles, and S. M. Block, "Stretching DNA with optical tweezers," Biophys. J. **72**, 1335–1346 (1997).
4. E. Qu, H. L. Guo, C. H. Xu, Z. L. Li, M. Yuan, B. Y. Cheng, and D. Z. Zhang, "Kinetics of microtubule -AtMAP65-1 bond studied with dual-optical tweezers," Jpn. J. Appl. Phys. **46**, 7514–7518 (2007).
5. A. K. Rai, A. Rai, A. J. Ramaiya, R. Jha, and R. Mallik, "Molecular adaptations allow dynein to generate large collective forces inside cells," Cell **152**, 172–182 (2013).
6. J. C. Crocker and D. G. Grier, "Microscopic measurement of the pair interaction potential of charge-stabilized colloid," Phys. Rev. Lett. **73**, 352–355 (1994).
7. G. M. Wang, E. M. Sevick, E. Mittag, D. J. Searles, and D. J. Evans, "Experimental demonstration of violations of the second law of thermodynamics for small systems and short time scales," Phys. Rev. Lett. **89**, 050601 (2002).
8. J. Köhler, R. Ghadiri, S. I. Ksouri, Q. Guo, E. L. Gurevich, and A. Ostendorf, "Generation of microfluidic flow using an optically assembled and magnetically driven microrotor," J. Phys. D **47**, 505501 (2014).
9. G. B. Liao, P. B. Bareil, Y. L. Sheng, and A. Chiou, "One-dimensional jumping optical tweezers for optical stretching of bi-concave human red blood cells," Opt. Express **16**, 1996–2004 (2008).
10. S. Mohanty, "Optically-actuated translational and rotational motion at the microscale for microfluidic manipulation and characterization," Lab Chip **12**, 3624–3636 (2012).
11. L. Lin, H. L. Guo, X. L. Zhong, L. Huang, J. F. Li, L. Gan, and Z. Y. Li, "Manipulation of gold nanorods with dual-optical tweezers for surface plasmon resonance control," Nanotechnology **23**, 215302 (2012).
12. L. Huang, H. L. Guo, K. L. Li, Y. H. Chen, B. H. Feng, and Z. Y. Li, "Three dimensional force detection of gold nanoparticles using backscattered light detection," J. Appl. Phys. **113**, 113103 (2013).
13. M. E. J. Friese, T. A. Nieminen, N. R. Heckenberg, and H. Rubinsztein-Dunlop, "Optical alignment and spinning of laser-trapped microscopic particles," Nature **395**, 621–635 (1998).
14. N. J. Jenness, R. M. Erb, B. B. Yellen, and R. L. Clark, "Magnetic and optical manipulation of spherical metal-coated Janus particles," Proc. SPIE **7762**, 776227 (2010).
15. H. Wang, S. Bhaskar, J. Lahann, and Y. G. Lee, "Optical trapping of Janus particles," Proc. SPIE **7038**, 703813 (2008).
16. S. Nedev, S. Carretero-Palacios, P. Kühler, T. Lohmüller, A. S. Urban, L. J. E. Anderson, and J. Feldmann, "An optically controlled microscale elevator using plasmonic Janus particles," ACS Photonics **2**, 491–496 (2015).
17. F. S. Merkt, A. Erbe, and P. Leiderer, "Capped colloids as light-mills in optical traps," New J. Phys. **8**, 216 (2006).
18. L. Baraban, R. Streubel, D. Makarov, L. Han, D. Karnaushenko, O. G. Schmidt, and G. Cuniberti, "Fuel-free locomotion of Janus motors: magnetically induced thermophoresis," ACS Nano **7**, 1360–1367 (2013).
19. M. Yoshida and J. Lahann, "Smart nanomaterials," ACS Nano **2**, 1101–1107 (2008).
20. T. Nisisako, T. Torii, T. Takahashi, and Y. Takizawa, "Synthesis of monodisperse bicolored Janus particles with electrical anisotropy using a microfluidic co-flow system," Adv. Mater. **18**, 1152–1156 (2006).
21. C. J. Behrend, J. N. Anker, B. H. McNaughton, and R. Kopelman, "Microrheology with modulated optical nanoprobes (MOONs)," J. Magn. Magn. Mater. **293**, 663–670 (2005).
22. D. A. White, "Vector finite element modeling of optical tweezers," Comput. Phys. Comm. **128**, 558–564 (2000).
23. D. C. Benito, S. H. Simpson, and S. Hanna, "FDTD simulations of forces on particles during holographic assembly," Opt. Express **16**, 2942–2957 (2008).
24. J. Q. Qin, X. L. Wang, D. Jia, J. Chen, Y. X. Fan, J. P. Ding, and H. T. Wang, "FDTD approach to optical forces of tightly focused

vector beams on metal particles," Opt. Express **17**, 8407–8416 (2009).

25. S. H. Simpson and S. Hanna, "Application of the discrete dipole approximation to optical trapping calculations of inhomogeneous and anisotropic particles," Opt. Express **19**, 16526–16541 (2011).
26. L. Lin, F. Zhou, L. Huang, and Z. Y. Li, "Optical forces on arbitrary shaped particles in optical tweezers," J. Appl. Phys. **108**, 073110 (2010).

27. F. Borghese, P. Denti, and R. Saija, "Radiation torque and force on optically trapped linear nanostructures," Phys. Rev. Lett. **100**, 163903 (2008).
28. A. Ashkin, "Forces of a single-beam gradient laser trap on a dielectric sphere in the ray optics regime," Biophys. J. **61**, 569–582 (1992).
29. M. Born and E. Wolf, *Principles of Optics*, 7th ed. (Cambridge University, 1999), pp. 54–59 and 628–633.